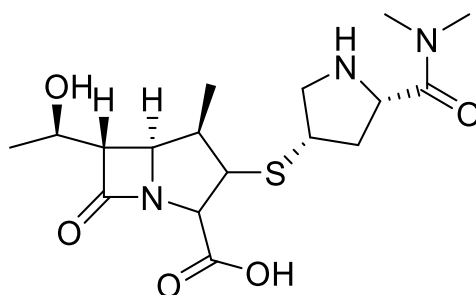


## STUDY ON THE ADSORPTION OF MEROPENEM ON MAGNETIC $\text{CoFe}_2\text{O}_4/\text{Au}$ COMPOSITE

HOANG THI HIEU <sup>(1)</sup>, NGUYEN THU PHUONG <sup>(1)</sup>, BUI THI TRIEU XUAN <sup>(1)</sup>,  
PHAM DUC THANG <sup>(2)</sup>, PHAM THI NGOC MAI <sup>(1)</sup>

### 1. INTRODUCTION

Meropenem (Fig. 1) is the pyrrolidinyl dimethyl carbamoyl derivative of thienamycin taken from streptomyces cattleya. It is considered as one of the injectable antibiotics which currently have the broadest antibacterial spectrum in the carbapenem group [1].



**Figure 1.** Structural formula of meropenem

Meropenem was indeed introduced to therapeutic areas as the strongest antibiotics to kill harmful microorganisms which are resistant to penicillin and cephalosporin antibiotics. Particularly, the carbapenems have been used as the last-resort antibiotics for patients in cases of infectious diseases and intensive care units who are seriously infected and/or multidrug-resistant. So far, the analogues of carbapenems in biological and pharmaceutical matrices have mostly been determined with common separation methods include liquid-liquid extraction, solid-liquid extraction (SPE), however they all ask for several steps and the selectivity towards analytes is still limited. Sample treatment coupled with magnetic nanoparticles can provide faster phase separation by applying an external magnetic field and be easy to reuse. To enhance the separation efficacy, magnetic particles have been surfaced functionalized with small organic molecules, polymer, aptamer, antibody and nano metal particles [2].

Among magnetic materials,  $\text{CoFe}_2\text{O}_4$  nanoparticles are widely used thanks to large anisotropy, high coercive field, moderate saturation magnetization, chemical stability and good electrical conductivity [3, 4]. The structure of the core-shell of iron-gold attracted much attention due to the obvious benefits of gold nanoparticles. Gold is an inert element and useful to be a coating material for protecting magnetic nanoparticles. Moreover, gold is very popular for its versatility in surface modification, high catalytic properties, unique biocompatibility and high affinity to sulfur or nitrogen containing compounds [5].

In this study, a composite  $\text{CoFe}_2\text{O}_4@\text{Au}$  was synthesized and applied for the effective adsorption of meropenem, which can be later used for separation and enrichment of meropenem from complicated matrices. The nano adsorbent material contains nano gold particles that have high adsorption towards meropenem thanks to high affinity between S atom in meropenem structure and Au surface; and the  $\text{CoFe}_2\text{O}_4$  core that helps to easily collect materials from sample solution [6]. Here in our study, the nano gold particles were synthesized by reducing  $\text{HAuCl}_4$  by  $\text{NaBH}_4$  in the presence of PDADMAC (a polycation polymer) as stabilizer instead of using the conventional citrate. To our knowledge, there is yet no researches that conduct on the using of PDADMAC as stabilizer for gold nano particles as well as the study of adsorption behavior of meropenem on  $\text{CoFe}_2\text{O}_4@\text{Au}$ .

## 2. MATERIALS AND METHODS

### 2.1. Materials

All chemicals used in the experiments are of analytical grade: Meropenem sodium salt 98% (Toronto Research Chemicals, Canada), chloroauric acid tetrahydrate ( $\text{HAuCl}_4 \cdot 4\text{H}_2\text{O}$ ), sodium borohydride ( $\text{NaBH}_4$ ), sodium hydroxide, potassium hydroxide hydrochloric acid (37%) (Merck, Germany), Poly (diallyldimethylammonium chloride) solution with molecular weight of 400-500kg/mol (PDADMAC 20wt.% in  $\text{H}_2\text{O}$ ,  $\text{Fe}(\text{NO}_3)_3 \cdot 9\text{H}_2\text{O}$ ,  $\text{Co}(\text{NO}_3)_2 \cdot 6\text{H}_2\text{O}$ , (3-Aminopropyl) triethoxysilane (APTES) (Sigma-Aldrich). Deionized water was used for preparing all the solutions for the experiments.

### 2.2. Meropenem determination by UV-Vis measurements

The concentrations of meropenem antibiotic before and after adsorption on  $\text{CoFe}_2\text{O}_4@\text{Au}$  material are determined by the UV-Vis spectrophotometer using the quartz cuvettes with a path length of 1 cm at the Analytical Chemistry department, Faculty of Chemistry, VNU University of Science. A series of standard concentrations of meropenem in the range of 1-25 mg/L is prepared in 25 mL volumetric flasks, and then filled up to the mark by double-distilled water. After that, the calibration curve of meropenem was constructed by measuring at the absorption maxima wavelength of 298 nm.

### 2.3. Synthesis of materials

#### 2.3.1. Synthesis of $\text{CoFe}_2\text{O}_4$ nanoparticles

Powdered ferromagnetic CFO materials were synthesized by hydrothermal method. Solution containing  $\text{Co}(\text{NO}_3)_2 \cdot 6\text{H}_2\text{O}$  and  $\text{Fe}(\text{NO}_3)_3 \cdot 9\text{H}_2\text{O}$  with the molar ratio of  $\text{Co}^{2+}$ :  $\text{Fe}^{3+}$  of 1: 2.2 were added in a beaker. Then pH solution was adjusted to 12 by using a pH meter. The obtained mixture was transferred to a thermo-hydrolysis vessel and hydrolyzed at  $150^\circ\text{C}$  and for 2-hours. After being hydrolyzed, the sample was taken out and washed several times with distilled and then filtered. Finally, the precipitate was dried at  $80^\circ\text{C}$  to produce  $\text{CoFe}_2\text{O}_4$  product as a black powder. The crystal structure and microstructure of obtained  $\text{CoFe}_2\text{O}_4$  was investigated by XRD measurement (using an X-ray diffractometer D8 Advance (Bruker, Germany) with the wavelength  $\text{Cu}_{K\alpha} = 1.5406 \text{ \AA}$  and  $2\theta$  angle of  $20^\circ$  to

80°) and FE-SEM measurement (using an ultra-high resolution field emission scanning electron microscopy FE-SEM S-4800 (Hitachi, Japan) with accelerated voltage up to 15 kV), respectively.

### 2.3.2. Synthesis of $\text{CoFe}_2\text{O}_4@\text{Au}$ composites

The Au nano particles were synthesized by reducing  $\text{HauCl}_4$  by  $\text{NaBH}_4$  in the presence of PDADMAC (a polycation polymer) as stabilizer. The freshly prepared dispersion of  $\text{CoFe}_2\text{O}_4$  (50 mg in 50 ml of water) was acidified with 0.1M of HCl at pH 6.5. While continuous stirring, successively 152 $\mu\text{L}$  of (3-Aminopropyl) triethoxysilane (APTES) and 200 $\mu\text{L}$  of 50mM  $\text{HAuCl}_4$  were added. 20 $\mu\text{L}$  of PDADMAC was added into the formed dark brown colloidal nanoparticle solution and the mixture was stirred for 10 minutes. After that, 2mL of a freshly prepared solution of  $\text{NaBH}_4$  (0.05 M) was added dropwise into the formed reddish brown colloidal nanoparticle solution, and then the mixture was stirred for three hours. The obtained substance was precipitated by centrifugation (5000 rev/min, for 20 min), washed with water and alcohol, and then it was dried 80°C for 12 hours. The obtained composite nanoparticles composed of magnetite and gold actively responded to an applied external magnetic field.

### 2.3.3. Batch adsorption of Meropenem on $\text{CoFe}_2\text{O}_4@\text{Au}$

To evaluate the capacity adsorption, the adsorbent (0.03-0.1g) was contacted with 10 mL of meropenem solutions (pH 3÷8) having initial concentrations ranging from 10, 25 and 40 mg/L in 25-mL falcon tubes. The falcon tubes were then shaken for 60 to 300 minutes. The concentrations of meropenem after adsorption were determined by using UV-Vis spectrophotometer.

The adsorption capacity  $q_e$  (mg/g) of meropenem onto  $\text{CoFe}_2\text{O}_4@\text{Au}$  was calculated by equation:

$$q_e = \frac{C_0 - C_e}{m} \cdot V \quad (1)$$

where  $C_0$  (mg/L) and  $C_e$  (mg/L) are the initial concentration and final concentration of meropenem, respectively,  $V$ (L) is the volume of the solution, and  $m$  (g) is the mass of the material.

For adsorption isotherms, Langmuir and Freundlich models were investigated. The linear form of Langmuir equation is:

$$\frac{q_e}{C_e} = \frac{C_e}{q_m} + \frac{1}{q_m K_L} \quad (2)$$

where  $q_e$  and  $q_m$  are equilibrium adsorption capacity (mg/g) and maximum adsorption capacity (mg/g), respectively and  $K_L$  is Langmuir adsorption constant (L/mg).

The linear form of the Freundlich model can be written as:

$$\log q_e = \log k_f + \frac{1}{n} \log C_e \quad (3)$$

where  $k_f$  is Freundlich adsorption capacity (L/g) and  $n$  is adsorption strength.

### 3. RESULTS AND DISCUSSION

#### 3.1. Characterization of $\text{CoFe}_2\text{O}_4$

The XRD pattern of  $\text{CoFe}_2\text{O}_4$  (CFO) is presented in Fig. 2, showing the diffraction peaks at  $2\theta = 30.1, 35.4, 43.3, 53.6, 57.5$  and  $63.0^\circ$ , which correspond to (220), (311), (111), (422), (511) and (440) planes. Comparing this result with the standard XRD data of CFO, we can see that all peaks belong to cubic spinel structure. It indicated that CFO phase has been formed in the hydrothermal process and the sample is single phase.

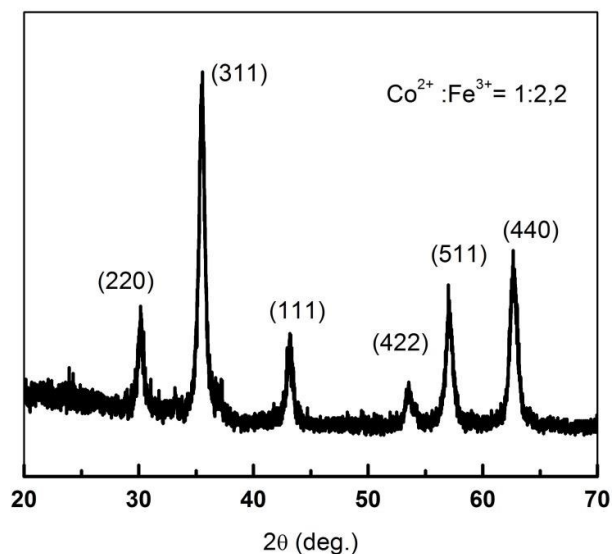


**Figure 2.** XRD pattern of CFO

The microstructure of the fabricated CFO sample was revealed in FE-SEM image provided in Fig. 3. CFO particles are spherical, quite uniform with the particle size ranging from 10 to 20 nm.

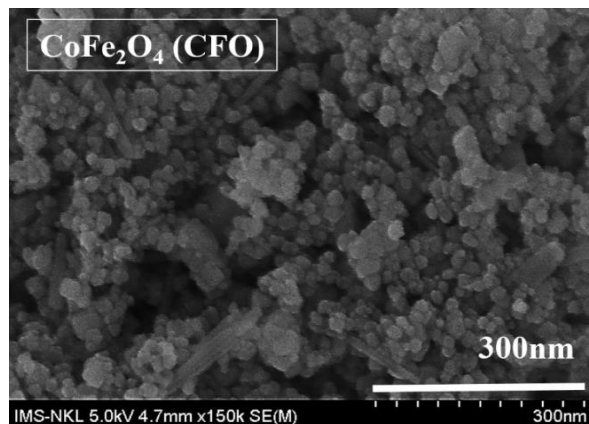


**Figure 3.** FE-SEM image of CFO sample

### 3.2. Batch adsorption of Meropenem on CoFe<sub>2</sub>O<sub>4</sub>@Au

#### 3.2.1. Effect of pH

pH is usually a factor that can greatly affect the adsorption of materials especially those have charge dependent on pH. The influence of the pH medium on the adsorption capacity of C18, CoFe<sub>2</sub>O<sub>4</sub>, and CoFe<sub>2</sub>O<sub>4</sub>@Au materials was investigated using 10.00 mL of 10 ppm Meropenem solution with pH varying from 3 to 8. As can be seen from Fig. 4, out of the three materials, the equilibrium adsorption capacity on CoFe<sub>2</sub>O<sub>4</sub>@Au at pH 6 was highest. Since gold has strong affinity towards -SH group in meropenem structure, meropenem is easily adsorbed on gold surface. Therefore, the adsorption capacity of nano composite CoFe<sub>2</sub>O<sub>4</sub>@Au is much higher than single CoFe<sub>2</sub>O<sub>4</sub> and C18, which adsorb meropenem only through weak Vanderwaal interaction (C18) or through hydroxyl functional groups on CoFe<sub>2</sub>O<sub>4</sub> surface.

The highest  $q_e$  was obtained for CoFe<sub>2</sub>O<sub>4</sub> at pH = 3, but still 2 times lower than maximum  $q_e$  obtained of CoFe<sub>2</sub>O<sub>4</sub>@Au. The common adsorbent C18 has poor adsorption capacity towards meropenem at all pH. For CoFe<sub>2</sub>O<sub>4</sub>@Au, when pH of solution increases from 3 to 6, the adsorption capacity tends to increase and reaches the maximum at pH 6, then decrease later with further increasing pH from 6 to 8. The maximum adsorption at pH 6, which lies around the isoelectric point (pI~6) of meropenem suggests the dominant contribution of hydrophobic interaction between meropenem and PDADMAC capping of AuNPs in comparison with the electrostatic interaction.

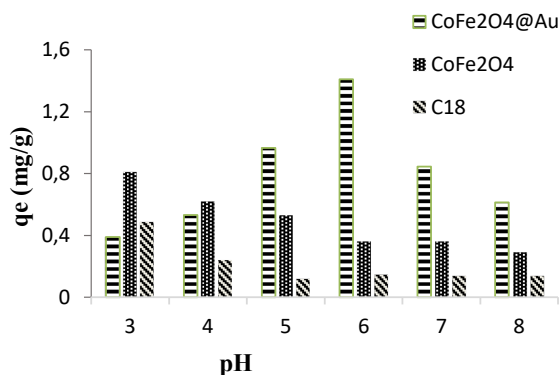


**Figure 4.** The effect of pH on the adsorption capacity of C18, CoFe<sub>2</sub>O<sub>4</sub>, and CoFe<sub>2</sub>O<sub>4</sub>@Au materials

#### 3.2.2. Effect of adsorbent mass

As the mass of CoFe<sub>2</sub>O<sub>4</sub>@Au was varied from 0.03g to 0.1g, the adsorption capacity increases and tends to get maximum at 0.05g. The increase of adsorption capacity with increasing adsorbent mass can be explained by the increase of the number of adsorption centers. However, when the mass of the material is above a certain amount, the adsorption capacity will reach saturation and even tend to decrease slightly. In the next experiments, the optimal adsorbent mass was selected as 0.05g.

### 3.2.3. Effect of NaCl concentration

Ionic strength usually strongly influences the double charge layer at adsorbent surface, hence strongly affects the adsorption capacity in the case of electrostatic interaction. Strong electrolyte NaCl with concentrations varying from  $7.5 \times 10^{-3}$  M to 0.75 M was added in  $\text{CoFe}_2\text{O}_4@\text{Au}$  solution in the presence of meropenem 25.00 ppm. Interestingly, the concentration of NaCl has slight effect on the adsorption capacity of meropenem, which once again reveals the less important effect of electrostatic interaction between meropenem and  $\text{CoFe}_2\text{O}_4@\text{Au}$ -PDADMAC adsorbent. Only with increasing the concentration of NaCl in the range from  $7.5 \times 10^{-3}$  M to 0.75 M, the adsorption capacity decreases slowly and tends to saturate at 0.5 M NaCl.

### 3.2.4. Effect of adsorption time

The effect of adsorption time on the adsorption behavior of meropenem on  $\text{CoFe}_2\text{O}_4@\text{Au}$  was investigated in the range from 0 to 300 min, at three initial Meropenem concentrations of 10.00 ppm, 25.00 ppm and 40.00 ppm. Results show that the uptake of meropenem ( $q_t$ ) (mg/g) increased with increasing adsorption time and remained nearly constant after 180 min. The amount of meropenem adsorbed ( $q_t$ ) at equilibrium increased from 1.83; 2.34 and 3.27 mg/g as the meropenem concentration increased from 10.00; 25.00 and 40.00 ppm, respectively.

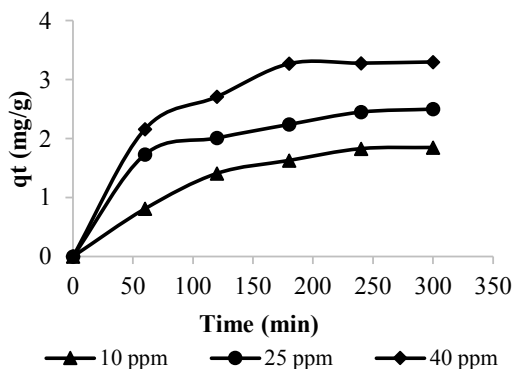


**Figure 5.** Effect of adsorption time on kinetic adsorption

The adsorption is rapid in the initial stages and gradually decreases with progress of adsorption (Fig. 5). All plots are single, smooth and continuous curves leading to saturation, suggesting the possible monolayer coverage of meropenem on the surface of the adsorbent.

### 3.2.5. Effect of initial meropenem concentrations

In static adsorption process, initial meropenem concentration in the solution plays an important role as the movement of the constituents in solution obeys the mass transfer process between the solution and the adsorbent surface. Systematical investigation on the initial meropenem concentration was further carried out in a wide concentration range from 10.00 ppm to 100.00 ppm.

As can be seen from Fig. 6, the equilibrium adsorption capacity of meropenem increases significantly at initial meropenem concentrations from 10 to 40 ppm, reaches a maximum of 3.27 mg/g at 40 ppm then tends to saturate at concentrations higher than 40 ppm. The obtained data will be further used to deduce the adsorption isotherms of meropenem on  $\text{CoFe}_2\text{O}_4@\text{Au}$ .

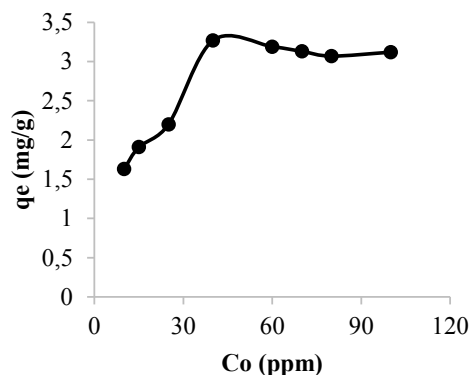


**Figure 6.** Effect of initial concentration of Meropenem on the adsorption capacity of the material

### 3.3. Study on the adsorption isotherms

For adsorption isotherms, Langmuir and Freundlich models are often applied in many cases. The Langmuir model describes the adsorption of molecules on a solid surface to gas pressure or concentration of a medium above the solid surface at a fixed temperature. It suggests that the adsorption process occurs in monolayers of the adsorbent surface. The Freundlich model is used for characterizing the adsorption which entails the heterogeneity of solid adsorbent surface interacting with an adsorbate.

As can be seen in Fig. 5,  $\log q_e$  does not linearly depend on  $\log C_e$ , with the correlation coefficient of 0.8743 much lower than 1 (Fig. 7), indicating the inconsistency of experimental results with the theoretical model Freundlich. Meanwhile, the highly linear dependence of  $C/q$  versus  $C_0$ , (Fig. 8) with a correlation coefficient of 0.9832, proves the agreement of the experimental results with the Langmuir theoretical model and the monolayer isothermal adsorption of Meropenem on  $\text{CoFe}_2\text{O}_4@\text{Au}$  material.

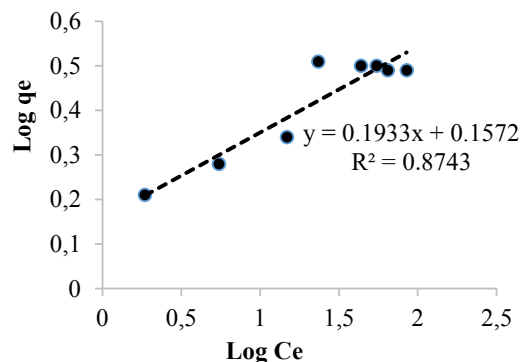


**Figure 7.** The dependence of  $\log q_e$  on the  $\log C_e$

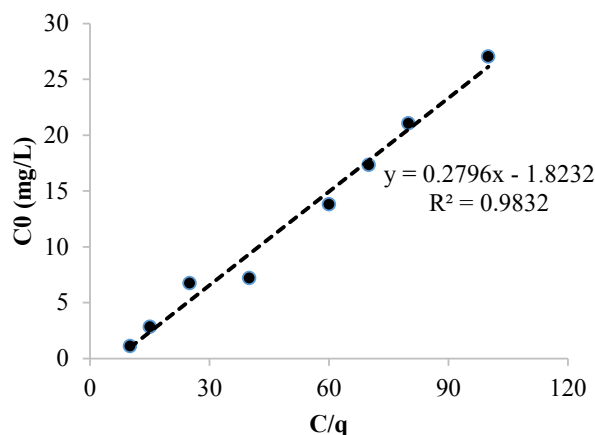


**Figure 8.** The dependence of  $C_0$  on  $C/q$

#### 4. CONCLUSIONS

We have successfully synthesized magnetic  $\text{CoFe}_2\text{O}_4@\text{Au}$  material having selective adsorption towards meropenem, which can be used for separation and enrichment of meropenem from aqueous solution. The optimum conditions for adsorption of Meropenem on  $\text{CoFe}_2\text{O}_4@\text{Au}$  were found to be pH 6, adsorption time 180 minutes, adsorbent mass 0.05g. The adsorption isotherm of meropenem  $\text{CoFe}_2\text{O}_4@\text{Au}$  follows well Langmuir theoretical model. The  $\text{CoFe}_2\text{O}_4@\text{Au}$  composite material also can be a potential candidate for other applications such as biological separation, target drug delivery, and biosensor.

#### REFERENCES

1. Zhanel, George G., et al., *Comparative review of the carbapenems*, Drugs, 2007, **67**(7):1027-1052.
2. Chen, Chun-Hsien, et al., *Nanomaterial-based adsorbents and optical sensors for illicit drug analysis*, Journal of Food & Drug Analysis, 2020, **28**(4).
3. Ayyappan S., John Philip, and Baldev Raj., *A facile method to control the size and magnetic properties of  $\text{CoFe}_2\text{O}_4$  nanoparticles*, Materials Chemistry and Physics, 2009, **115**(2-3):712-717.
4. Shaterian, Maryam, et al., *Synthesis, characterization and electrochemical sensing application of  $\text{CoFe}_2\text{O}_4/\text{graphene}$  magnetic nanocomposite for analysis of atenolol*, Polyhedron, 2020, **182**:14479.
5. Karami, Changiz, and Mohammad Ali Taher, *A catechol biosensor based on immobilizing laccase to  $\text{Fe}_3\text{O}_4@\text{Au}$  core-shell nanoparticles*, International journal of biological macromolecules, 2019, **129**:84-90.
6. Baskakov A.O., et al., *Magnetic and interface properties of the core-shell  $\text{Fe}_3\text{O}_4/\text{Au}$  nanocomposites*, Applied surface science, 2017, **422**:638-644.



## SUMMARY

In this study, a magnetic core-shell  $\text{CoFe}_2\text{O}_4@\text{Au}$  was synthesized and applied for the effective adsorption of Meropenem, which can be later used for separation and enrichment of Meropenem from complicated matrices.  $\text{CoFe}_2\text{O}_4@\text{Au}$  exhibit better adsorption of meropenem than single phase  $\text{CoFe}_2\text{O}_4$  and conventional C18 adsorbent. Batch kinetic adsorption study revealed that the optimum conditions for Meropenem on  $\text{CoFe}_2\text{O}_4@\text{Au}$  were pH 6, adsorption time 180 minutes, adsorbent mass 0.05 g. The Meropenem adsorption isotherm was in accordance with Langmuir adsorption.

**Keywords:** Meropenem,  $\text{CoFe}_2\text{O}_4$ ,  $\text{CoFe}_2\text{O}_4@\text{Au}$ .

*Nhận bài ngày 20 tháng 5 năm 2021*

*Phản biện xong ngày 03 tháng 6 năm 2021*

*Hoàn thiện ngày 04 tháng 6 năm 2021*

<sup>(1)</sup> Faculty of Chemistry, VNU University of Science

<sup>(2)</sup> Faculty of Materials Science and Engineering, Phenikaa University Nano Institute, Phenikaa University